

The Nature of Heavy Quasiparticles in Magnetically Ordered Heavy Fermions

M. Dressel^{1*}, N. Kasper¹, K. Petukhov¹, B. Gorshunov¹, G. Grüner², M. Huth³, and H. Adrian³

¹*Physikalisches Institut, Universität Stuttgart, Pfaffenwaldring 57, D-70550 Stuttgart, Germany*

²*Department of Physics, University of California, Los Angeles, CA, 90095-1547*

³*Institut für Physik, Universität Mainz, D-55099 Mainz, Germany*

(Received November 13, 2018)

The optical conductivity of the heavy fermions UPd_2Al_3 and UPt_3 has been measured in the frequency range from 10 GHz to 1.2 THz (0.04 meV to 5 meV) at temperatures $1 \text{ K} < T < 300 \text{ K}$. In both compounds a well pronounced pseudogap of less than a meV develops in the optical response at low temperatures; we relate this to the antiferromagnetic ordering. From the energy dependence of the effective electronic mass and scattering rate we derive the energies essential for the heavy quasiparticle. We find that the enhancement of the mass mainly occurs below the energy which is related to magnetic correlations between the local magnetic moments and the itinerant electrons. This implies that the magnetic order in these compounds is the pre-requisite to the formation of the heavy quasiparticle and eventually of superconductivity.

PACS numbers: 71.27.+a, 78.20.-e, 74.70.Tx, 72.15.Qm

In common metals itinerant electrons of the conduction band are responsible for the electrical transport. The conductivity is frequency independent until the scattering with phonons and imperfections leads to a drop in the real part of the optical conductivity $\sigma_1(\omega)$ around the scattering frequency Γ . This behaviour is well described by the Drude model: $\hat{\sigma}(\omega) = \sigma_1 + i\sigma_2 = (Ne^2/m)/(\Gamma - i\omega)$ with the charge carrier mass m and scattering rate Γ assumed to be frequency independent. Here N is the carrier concentration, e is the electronic charge, and ω is the frequency [1]. While at room temperature also heavy-fermion metals follow this scenario, at liquid-helium temperatures large deviations are observed which are caused by many-body effects.

Heavy fermions show an unusual interplay of electronic correlations due to an interaction of itinerant electrons and local magnetic moments. At low temperatures these intermetallic compounds exhibit significant increase of the magnetic susceptibility and the electronic contribution to the specific heat compared to most metals. This is commonly explained by an enhanced effective mass m^* of some hundred times the free electron mass due to the highly correlated electronic behaviour and is described in the context of interacting Fermi liquids [2]. The strong interaction of the quasi-free conduction-band electrons with nearly localized f -electrons leads to a many-body resonance, i.e., an enhanced density of states at the Fermi energy [3]. The pile-up of this narrow resonance sets in below the so-called coherence temperature T^* , which is experimentally determined by a drop in the dc-resistivity and a cusp in the susceptibility, and typically is between 10 and 100 K.

Also the optical properties show clear signatures of the coherent many-body ground state: As a consequence of the large effective mass m^* the spectral weight $\int \sigma_1(\omega) d\omega = \omega_p^{*2}/8$ is reduced. $\omega_p^* = (\frac{4\pi Ne^2}{m^*})^{1/2}$ is called the renormalized plasma frequency. The relevant elec-

tronic excitations shift to very low energies, best characterized by an effective scattering rate Γ^* [4]. With decreasing temperature the electronic correlations become more pronounced, leading to a gradual increase of the effective mass m^* and the corresponding decrease of the effective scattering rate. The interaction of the conduction electron spins with the atomic moments in the heavy-fermion crystals explains the reduction of the magnetic susceptibility and also leads to a hybridization gap Δ in the density of states. The gap scales with the coherence temperature $(\Delta/T^*)^2 = m/m^*$ and is commonly observed in the far infrared range of frequency [5,6]. Using a frequency dependent scattering rate and effective mass for the description of the optical properties of correlated electron systems one obtains the energy dependence of the renormalization effects which goes beyond the information derived from static thermodynamic measurements. In the low-energy limit the frequency dependence of both parameters $m^*(\omega)$ and $\Gamma(\omega)$ should resemble their temperature dependence [1].

An additional aspect becomes important for those heavy-fermion compounds which undergo a magnetic phase transition. Antiferromagnetism is often due to the ordering of localized magnetic moments; this commensurate magnetic structure does not lead to a gap at the Fermi energy. In the case of a spin density wave, a spatial density modulation of the spin direction of the conduction electrons leads to antiferromagnetism, which in general is incommensurate with the underlying lattice; a gap in the electronic density of states at the Fermi energy is observed. Optical experiments exhibit a clear gap feature in the latter case while for the first case we expect no influence on the optical properties [7].

Because of its two-component electronic character, UPd_2Al_3 exhibits both pronounced local magnetic moment and heavy-fermion itinerant behaviour [8–10]. The 5f-shell has an average occupation of slightly less than

three, with two electrons localized in the U^{4+} state and the remaining $5f$ -electrons considered to be itinerant due to their large hybridization with the conduction electrons [11]. This coexistence is seen in the large magnetic moment ($0.85 \mu_B$) well below the antiferromagnetic ordering temperature $T_N \approx 14$ K which is almost atomic-like, while at the same time the itinerant electrons display a large Sommerfeld coefficient of the electronic specific heat $\gamma = 140 \text{ mJ mol}^{-1}\text{K}^{-2}$ which indicates an effective mass $m^*/m \approx 50$. The magnetic ordering is of local origin and the formation of a spin density wave can be ruled out [7,12]. The heavy quasiparticles condense in the superconducting state below $T_c \approx 2$ K. In order to reconcile magnetic ordering and superconductivity it was first suggested that different parts of the Fermi surface lead to antiferromagnetism and to the heavy-fermion ground state. Recent observations by tunneling spectroscopy and inelastic neutron scattering indicate, however, that magnetic excitons produce the effective coupling between the itinerant electrons and are responsible for superconductivity in UPd_2Al_3 [13,14].

If there is an interaction between magnetic and electronic excitations in the superconducting state, the question arises, whether the magnetic ordering also affects the heavy quasiparticles in the normal state. In which way, or how far, is the low-temperature ground state (still $T > T_c$), where the large effective mass m^* has been determined, affected by the magnetic ordering? Are solely the electronic correlations of the f -shell electrons with the conduction-band electrons responsible for this enhancement as was argued above within the common heavy-fermion picture?

In order to address these questions, we have investigated the optical properties of UPd_2Al_3 in the frequency range from 10 GHz to 1.2 THz (0.3 to 40 cm^{-1} , corresponding to a photon energy of 0.04 to 5 meV) at temperatures $2 \text{ K} < T < 300 \text{ K}$. Using a Mach-Zehnder interferometer equipped with tunable, coherent radiation sources we measured the absorption and the phase shift of the radiation upon passing through a 150 nm thick epitaxial grown UPd_2Al_3 -film deposited on a LaAlO_3 substrate by molecular beam epitaxy [15]. In addition we performed microwave and millimeter wave experiments utilizing enclosed cavities [16]. Our data were supplemented with reflectivity measurements on bulk samples [7] in order to obtain the absorptivity over an extremely broad frequency range as plotted in Fig. 1a. The lines in this figure represent the input we used for the Kramers-Kronig analysis in order to obtain the optical conductivity. The result of it is plotted in the lower panel of Fig. 1; in addition we display the directly measured conductivity data. In the Kramers-Kronig analysis tried to fit both the absorptivity and the conductivity data best, taking the different experimental uncertainties into account [16].

The main findings can be summarized as follows: At high temperatures we observe a broad conductivity spec-

trum as expected for a Drude metal. As the temperature decreases below $T^* \approx 50$ K, a renormalized Drude peak develops due to the gradual enhancement of the effective mass m^* . At the same time, a gap feature develops around 100 cm^{-1} as expected from the hybridization of the localized $5f$ -electrons and the conduction electrons. This behaviour is typical for heavy fermions [4]. Lowering the temperature further, magnetic ordering sets in at T_N and leads to distinct signatures in the optical spectrum. In the magnetically ordered state we observe a well pronounced pseudogap below 2 cm^{-1} which we assign to the interaction of the localized magnetic moments and spins of the itinerant electrons. At even lower frequencies, an extremely narrow zero-frequency mode remains which is responsible for the dc conductivity and for superconductivity below T_c .

To describe the low-energy data satisfactorily, we introduce a complex frequency dependent scattering rate $\hat{\Gamma}(\omega) = \Gamma_1(\omega) + i\Gamma_2(\omega)$ into the standard Drude form of $\hat{\sigma}(\omega)$. With the dimensionless quantity $\lambda(\omega) = -\Gamma_2(\omega)/\omega$, the complex conductivity can be written as [1]

$$\hat{\sigma}(\omega) = \sigma_1 + i\sigma_2 = \frac{(\omega'_p)^2}{4\pi} \frac{1}{\Gamma_1(\omega) - i\omega(m^*(\omega)/m)} \quad (1)$$

where $m^*/m = 1 + \lambda(\omega)$ is the frequency dependent enhanced mass. $(\omega'_p)^2$ corresponds to the fraction of electrons which participate in the many-body state developing below T^* . By rearranging Eq. (1) we can write expressions for $\Gamma_1(\omega)$ and $m^*(\omega)$ in terms of $\sigma_1(\omega)$ and $\sigma_2(\omega)$ as follows:

$$\Gamma_1(\omega) = \frac{(\omega'_p)^2}{4\pi} \frac{\sigma_1(\omega)}{|\hat{\sigma}(\omega)|^2}, \quad (2)$$

$$\frac{m^*(\omega)}{m} = \frac{(\omega'_p)^2}{4\pi} \frac{\sigma_2(\omega)/\omega}{|\hat{\sigma}(\omega)|^2}. \quad (3)$$

Such analysis allows us to look for interactions which would lead to energy dependent renormalization as the frequency dependent scattering rate and effective mass are related to the real and imaginary parts of the energy dependent self-energy of the electrons [17]. In Fig. 2 the frequency dependences of the scattering rate $\Gamma_1(\omega)$ and the effective mass $m^*(\omega)$ are displayed for different temperatures. As expected for a normal metal, at $T > T^*$ the spectra of $\Gamma_1(\omega)$ and $m^*(\omega)$ are nearly frequency independent. As the temperature is lowered we observe a peak in the energy dependent scattering rate at the hybridization gap, as can be nicely seen in the $T = 30$ K data of Fig. 2b. The decrease of $\Gamma_1(\omega)$ to lower frequencies corresponds to an increase of $m^*(\omega)$. At these intermediate temperatures, $T_N < T < T^*$, the effective mass m^*/m gradually increases when going to smaller frequencies or correspondingly to lower temperatures; eventually it reaches a value of 35. Decreasing the

temperature below T_N results in a second peak of $\Gamma_1(\omega)$ and a strong increase of the effective mass below 1 cm^{-1} . As already seen at $T = 15 \text{ K}$, this effect becomes stronger as the temperature is lowered to 2 K . The effective mass $m^*(\omega)$ levels off at $m^*/m \approx 50$ below 1 cm^{-1} and nicely matches the values obtained by thermodynamic methods [8] which are indicated by the star in Fig. 2c. We see a moderate enhancement of $m^*(\omega, T \rightarrow 0)$ for frequency below the hybridization gap and a larger one below the gap which develops due to magnetic correlations. Accordingly $m^*(\omega \rightarrow 0, T)$ increases only slightly below T^* and shows a large enhancement below T_N . The scattering rate drops more than one order of magnitude upon passing T_N ; this can be explained by the freezing-out of spin-flip scattering in the ordered state. The energy-dependent scattering rate is related to the electronic density of states. In the case of UPd_2Al_3 we can distinguish two gap structures with an enhanced density of states at the edges, features known for superconductors.

The estimation of the reduced spectral weight $\omega_p^* = c/\lambda_L(0) \approx 4000 \text{ cm}^{-1}$ from the London penetration depth $\lambda_L = 450 \text{ nm}$ [9] agrees with our results of 4300 cm^{-1} if we integrate the conductivity spectrum up to 100 cm^{-1} ; a renormalized Drude behaviour without a gap feature would yield a value more than twice as large. This implies that all carriers seen in our low-energy spectra are in the heavy-fermion ground state and eventually undergo the superconducting transition below T_c . We can definitely rule out an assignment of the gap simply to the localized carriers of the antiferromagnetic ordered states, with the delocalized carriers contributing only to the narrow feature at $\omega = 0$, because its small spectral weight at low temperatures accounts for only 18 % of the carriers which become superconducting. This also means that the excitations above the gap stem from the delocalized states and that the gap observed in our conductivity spectra is related to exchange correlations of the second subsystem. Recently it was found that the magnetic excitations seen by neutron scattering produce effective interactions between itinerant electrons and lead to superconductivity [14]. Our results now imply that the magnetic excitations responsible for superconductivity also cause the heavy quasiparticles.

The picture we developed in order to explain the optical properties of UPd_2Al_3 should also apply to other heavy fermion compounds, in particular to UPt_3 which exhibits a similar behaviour in many regards [2,18]. For UPt_3 the effective mass of the quasiparticles is larger ($m^*/m \approx 200$) and the relevant energy scales are lower. The coherence temperature is $T^* \approx 30 \text{ K}$, fluctuating short range magnetic order ($0.02\mu_B$) occurs at $T_N = 5 \text{ K}$, and superconductivity sets in at $T_c = 0.5 \text{ K}$. Recent bandstructure calculations [19] infer the existence of localized as well as delocalized $5f$ -electrons in UPt_3 very much similar to UPd_2Al_3 . It was suggested that the observed enhancement of the quasiparticle mass results

from the local exchange interaction of two localized $5f$ -electrons with the remaining delocalized ones [19].

We have reanalyzed the optical properties of UPt_3 previously obtained by various techniques [20,21] in the same way as described above and can identify similar features (Fig. 3). When the coherent ground state builds up ($T < T^*$), the optical conductivity increases for frequencies below 30 cm^{-1} . As the temperature drops below $T_N = 5 \text{ K}$, magnetic ordering occurs and an energy gap progressively develops at about 3 cm^{-1} which is assigned to magnetic correlations [21]. The frequency dependence of the effective mass displayed in Fig. 3c clearly shows at the lowest temperature accessible that only a marginal increase of m^* is observed around 30 cm^{-1} , while below the energies related to the magnetic correlations the mass is drastically enhanced. Thus we also find that, as for UPd_2Al_3 , the coupling of the localized and delocalized $5f$ -electrons causes the heavy quasiparticles in UPt_3 ; these magnetic excitations are very likely to be responsible for superconductivity.

For both compounds, it therefore appears that the formation of the heavy quasiparticles relies on the establishment of antiferromagnetic order rather than competition of the coherent singlet formation and the magnetic order. Since we made similar observations for two materials which may have a different ground state as evidenced by the vastly different μ_B , it remains to be seen how far our findings have implications on non-magnetic heavy fermions with a large effective mass. Thermodynamic measurements should test our idea that the effective mass $m^*(T)$ increases only slightly below T^* but shows a large enhancement below T_N . It also remains to be seen in which way our observation is related to the pseudogap which was established in high-temperature superconductors well above T_c by optical and other methods [22].

In conclusion, the electrodynamic response of two uranium-based heavy fermion superconductors with magnetic ordering exhibits a behavior at low temperatures and low frequencies which cannot be explained within the simple picture of a renormalized Fermi liquid. The low-energy response shows the well-known renormalized behavior only above the magnetic ordering temperature; below T_N additional features were discovered. Besides an extremely narrow zero-frequency response, we observe a pseudogap of less than a meV. The experiments yield indications that this pseudogap is connected to magnetic correlations on the delocalized charge carriers. We have argued, that this gap at extremely low energies is due to the influence of the localized magnetic moments on the conduction electrons and this interaction is mainly responsible for the enhanced mass m^* .

We acknowledge helpful discussions with P. Fulde, A. Muramatsu, A. Schwartz, F. Steglich, and G. Zwicknagl. The work was supported by the DFG.

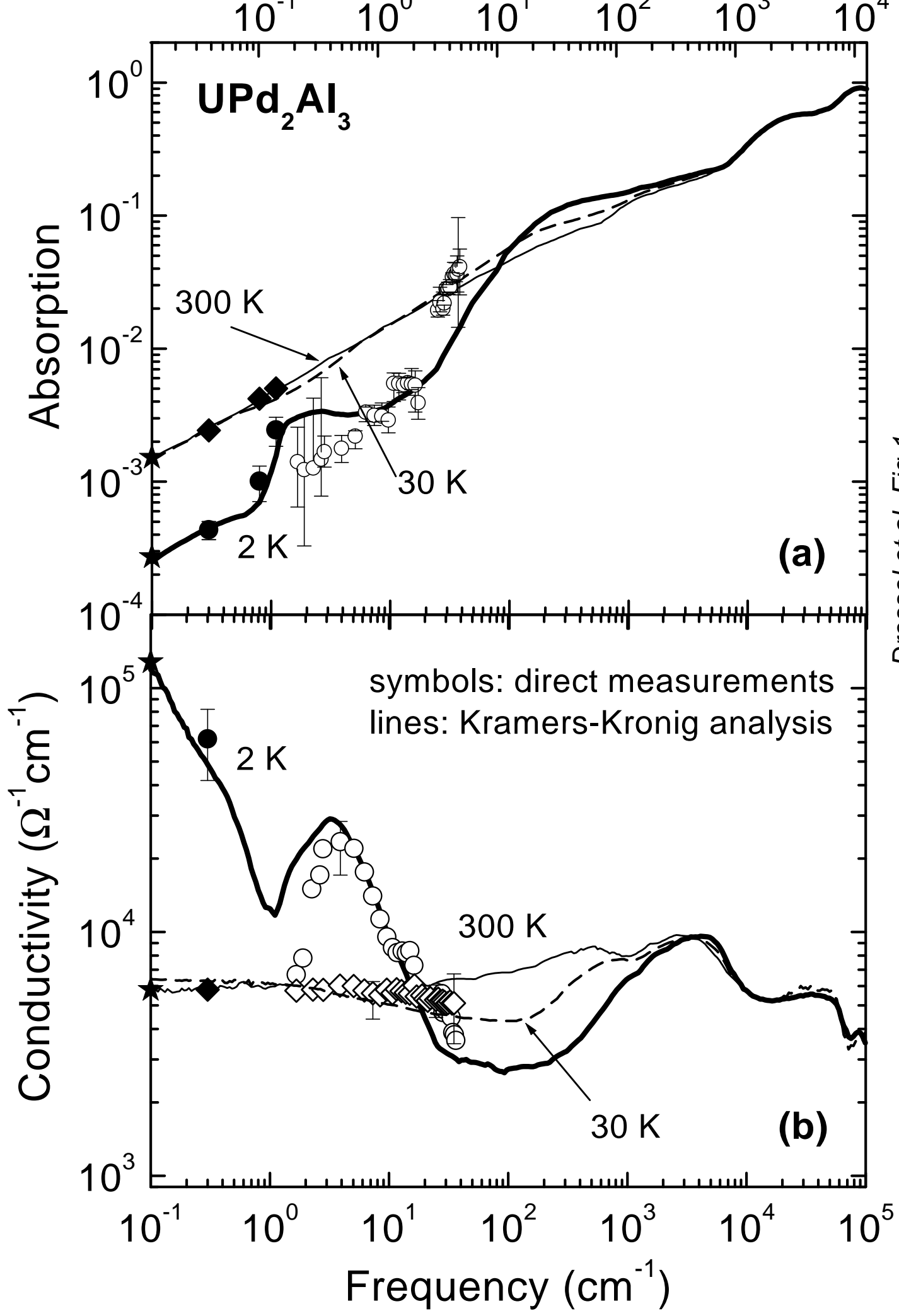
* email: dressel@pi1.physik.uni-stuttgart.de

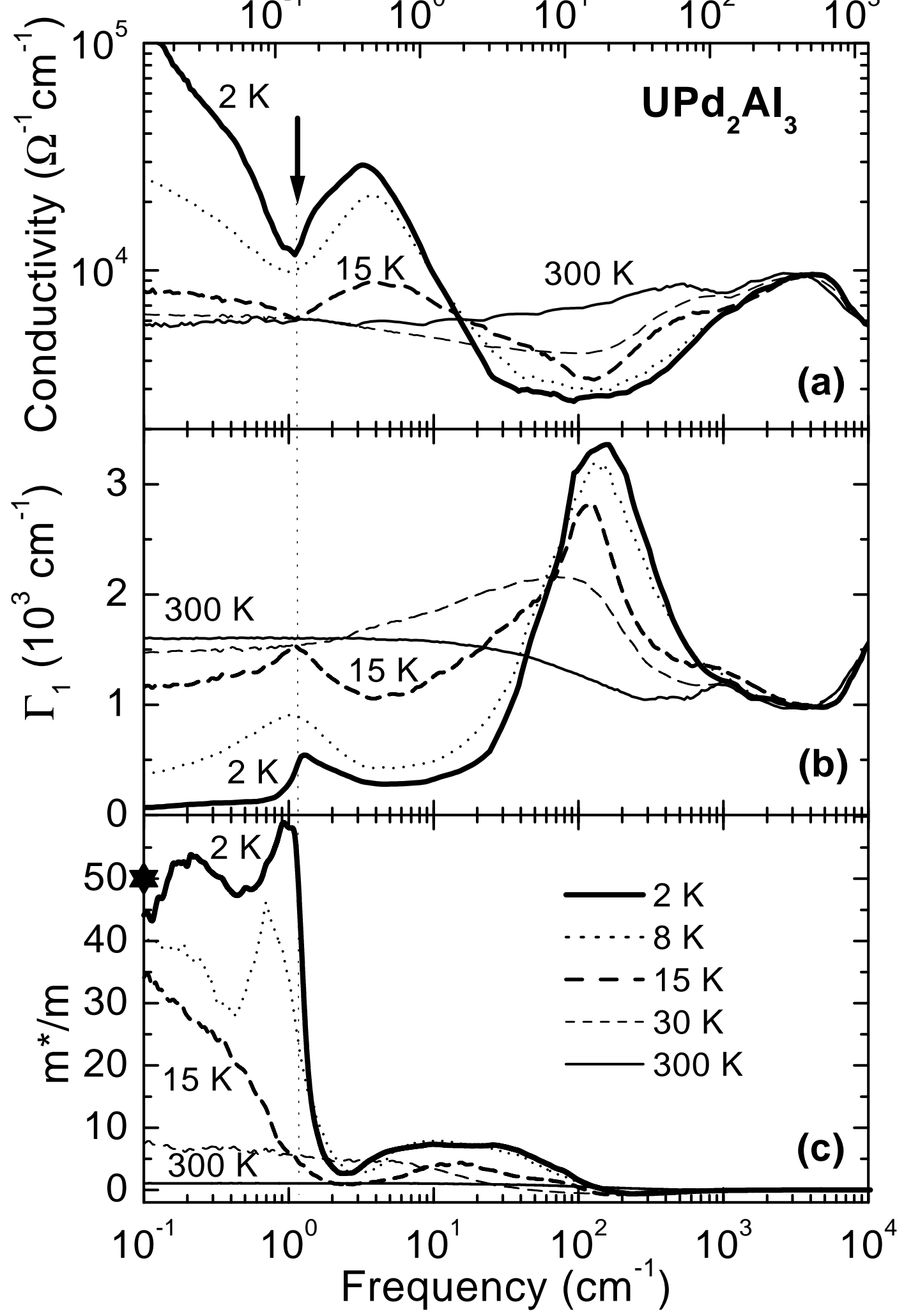
- [1] M. Dressel and G. Grüner, *Electrodynamics of Solids* (Cambridge University Press, Cambridge, 2002).
- [2] Z. Fisk *et al.*, Science **239**, 33 (1988).
- [3] N. Grewe and F. Steglich, in: *Handbook on the Physics and Chemistry of Rare Earths* **14**, ed. by K.A. Gschneider and L. Eyring (Elsevier, Amsterdam, 1991), p. 343.
- [4] L. Degiorgi, Rev. Mod. Phys. **71**, 687 (1999).
- [5] A.C. Hewson, *The Kondo Problem to Heavy Fermions* (Cambridge University Press, Cambridge, 1997).
- [6] S.V. Dordevic *et al.*, Phys. Rev. Lett. **86**, 684 (2001).
- [7] L. Degiorgi *et al.*, Z. Phys. B **102**, 367 (1997).
- [8] C. Geibel *et al.*, Z. Phys. B **84**, 1 (1991).
- [9] R. Caspary *et al.*, Phys. Rev. Lett. **71**, 2146 (1993).
- [10] R. Feyerherm *et al.*, Phys. Rev. Lett. **73**, 1849 (1994).
- [11] K. Knöpfle *et al.*, J. Phys.: Cond. Matter **8**, 901 (1996).
- [12] A. Krimmel *et al.*, J. Phys.: Cond. Matter **8**, 1677 (1996).
- [13] M. Jourdan *et al.*, Nature **398**, 47 (1999).
- [14] N.K. Sato *et al.*, Nature **410**, 340 (2001).
- [15] M. Huth *et al.*, Solid State Commun. **87**, 1133 (1993).
- [16] M. Dressel *et al.*, to be published.
- [17] A.A. Abrikosov *et al.*, *Quantum Field Theoretical Methods in Statistical Physics* (Pergamon, New York, 1965).
- [18] H.R. Ott, in: *Progress in Low Temperature Physics* **11**, ed. by D.F. Brewer (Elsevier, Amsterdam, 1987), p. 215.
- [19] G. Zwicknagl *et al.*, cond-mat/0107378.
- [20] P.E. Sulewski *et al.*, Phys. Rev. B **38**, 5338 (1988).
- [21] S. Donovan *et al.*, Phys. Rev. Lett. **79**, 1401 (1997).

FIG. 1. (a) Frequency dependent absorptivity of UPd₂Al₃ at different temperatures measured over a wide frequency range. The symbols on the left axis represent the dc values in a Hagen-Rubens behaviour; the full symbols in the microwave range are obtained by cavity perturbation technique; the open symbols present absorption evaluated from the transmission and phase measurement by the Mach-Zehnder interferometer (only 2 K data are plotted for clarity reasons). The lines are obtained by combining the various optical investigations (transmission through films and reflection of bulk samples). (b) Corresponding optical conductivity of UPd₂Al₃ as evaluated by a Kramers-Kronig analysis of the above absorption data. The data points on the left axis indicate the dc conductivity; the full symbols correspond to the direct determination of the optical conductivity using the transmission and the phase shift obtained by the Mach-Zehnder interferometer.

FIG. 2. Frequency dependence of (a) the optical conductivity $\sigma_1(\omega)$, (b) the scattering rate $\Gamma_1(\omega)$, and (c) the effective mass $m^*(\omega)$ of UPd₂Al₃ for different temperatures. The point on the left axis corresponds to the effective mass derived by thermodynamic measurements [8]. The arrow marks the correlation gap.

FIG. 3. Frequency dependence of (a) the optical conductivity $\sigma_1(\omega)$, (b) the scattering rate $\Gamma_1(\omega)$, and (c) the effective mass $m^*(\omega)$ of UPt₃ for different temperatures using the optical data obtained by [20,21].





Dressel et al. Fig. 2

